Backstepping control of the current profile in the DIII-D Tokamak

Mark D. Boyer[1], Justin Barton[1], Eugenio Schuster[1]
Michael Walker[2], David Humphreys[2]

[1]Department of Mechanical Engineering & Mechanics
Lehigh University

[2]General Atomics

m.dan.boyer@lehigh.edu

53rd Annual Meeting of the APS Division of Plasma Physics

This work was supported by the NSF CAREER Award Program (ECCS-0645086)
and the US DOE under DE-FG02-09ER55064 and DE-FC02-04ER54698

November 17, 2011

Overview

- A control oriented, first principles based model for the current profile evolution in DIII-D was developed
- We utilized a control design technique called backstepping in which a recursive transformation is used to calculate a feedback law for controlling the current profile
- The current profile control algorithm was implemented in the DIII-D Plasma Control System
- Simulations were performed to test the implementation code and tune the controller design
- Experimental tests of the controller were also done, showing results that are very similar to the simulations

The Need for Current Profile Control

- One of the challenges of tokamak fusion reactors is achieving operation with sufficiently long plasma discharges.
- Non-inductive sources of current are required for steady state-operation
- Setting up a suitable toroidal current profile can lead to self-generated, non-inductive current (bootstrap current)
- Controlling the current profile will therefore be important to achieving steady-state reactor operation
- The current profile can be actuated through
  - plasma current
  - neutral beams
  - radio frequency waves
  - plasma density

Approaches to Current Profile Modeling

- Linear plasma response modeling
  - Linear dynamic models of the current profile were identified at JET by performing system identification experiments [1].
  - These models are only valid in a region near the equilibrium around which they were identified.
  - To extend the control designs to other tokamaks, new system identification experiments have to be conducted on the other machines
- First principles based modeling
  - Derived from Gauss's law, Ampere's law, Faraday's law, Ohm's law, and an equilibrium momentum balance
  - Can be adapted to various tokamaks and equilibrium configurations.
  - Accounts for nonlinear coupling between magnetic and kinetic plasma profiles.
  - Explicitly describe the temporal and spatial evolution of the current profile.
  - Control strategies for various tokamaks can be synthesized from one model.

[1] D. Moreau et al., "A Two-time-scale Dynamic-model Approach for Magnetic and Kinetic Profile Control in Advanced Tokamak Scenarios on JET," *Nuclear Fusion*, 2008.

Approach to Current Profile Control

- Create desired current profile during the ramp-up and early flat-top phases of discharge then maintain target profile for remainder of discharge.
- First principles based control-oriented model of the current profile evolution was developed in [2].
- Control strategy: feedforward + feedback.
  - Feedforward: Computed off-line using nonlinear programming [3] and extremum seeking [4].
  - Feedback: Computed on-line and needed to regulate current profile around desired reference trajectories and reject external disturbances.
- In this work, we synthesize, simulate, and experimentally test a backstepping feedback control algorithm

[2] Y. Ou et al., "Towards Model-Based Current Profile Control at DIII- D," *Fusion Engineering and Design*, 2007.
[3] C. Xu et al., "Ramp-Up Phase Current Profile Control of Tokamak Plasmas via Nonlinear Programming," *IEEE Transactions on Plasma Science*, 2010.
[4] Y. Ou et al., "Design and Simulation of Extremum-Seeking Open-Loop Optimal Control of Current Profile in the DIII-D Tokamak," *Plasma Physics and Controlled Fusion*, 2008.

Current Profile Evolution Model

- Simplified scenario-oriented models for the electron temperature, the non-inductive current density, and the plasma resistivity were identified.
- These simplified models were then substituted into the first principles based magnetic diffusion equation governing the evolution of the poloidal flux profile $\psi(\hat{\rho}, t)$ [2] to obtain

$$\frac{\partial \psi}{\partial t} = f_1(\hat{\rho}) u_1(t) \frac{1}{\hat{\rho}} \frac{\partial}{\partial \hat{\rho}} \left(\hat{\rho} f_4(\hat{\rho}) \frac{\partial \psi}{\partial \hat{\rho}} \right) + f_2(\hat{\rho}) u_2(t) \tag{1}$$

with boundary conditions

$$\left. \frac{\partial \psi}{\partial \hat{\rho}} \right|_{\hat{\rho}=0} = 0 \qquad \left. \frac{\partial \psi}{\partial \hat{\rho}} \right|_{\hat{\rho}=1} = -k_3 u_3(t). \tag{2}$$

Note: $u_1(t)$, $u_2(t)$, and $u_3(t)$ are the control actuators which are nonlinear functions of:

- Total plasma current.
- Total non-inductive power (neutral beams).
- Line-averaged plasma density.

Current Profile Evolution Model - Flux Gradient

- The development of the bootstrap current is related to the shape of the q profile, which is proportional to $\partial\psi/\partial\hat{\rho}$
- We therefore define the variable of interest $\theta = \partial\psi/\partial\hat{\rho}$ and can arrive at the model

$$\frac{\partial\theta}{\partial t} = h_0(\hat{\rho})u_1\theta'' + h_1(\hat{\rho})u_1\theta' + h_2(\hat{\rho})u_1\theta + h_3(\hat{\rho})u_2 \tag{3}$$

with boundary conditions:

$$\theta\Big|_{\hat{\rho}=0} = 0 \qquad \theta\Big|_{\hat{\rho}=1} = -k_3u_3(t) \tag{4}$$

- Using feedforward inputs and nominal initial conditions, the system would satisfy

$$\frac{\partial\theta_{ff}}{\partial t} = h_0u_1\theta''_{ff} + h_1u_1\theta' + h_2u_1\theta + h_3u_2 \tag{5}$$

with boundary conditions:

$$\theta\Big|_{\hat{\rho}=0} = 0 \qquad \theta\Big|_{\hat{\rho}=1} = -k_3u_3(t) \tag{6}$$

Current Profile Evolution Model - Deviations

- In the presence of disturbances or perturbed initial conditions, an unwanted deviation $\tilde{\theta} = \theta - \theta_{ff}$ will exist.
- We can write the evolution of the deviations as

$$\frac{\partial \tilde{\theta}}{\partial t} = h_0 u_{1_{ff}} \tilde{\theta}'' + h_1 u_{1_{ff}} \tilde{\theta}' + h_2 u_{1_{ff}} \tilde{\theta} \tag{7}$$

with boundary conditions

$$\tilde{\theta}\Big|_{\hat{\rho}=0} = 0 \qquad \tilde{\theta}\Big|_{\hat{\rho}=1} = -k_3 u_{3_{fb}} \tag{8}$$

- Note that we have included the term $u_{3\,fb}$ to allow us to include feedback in the control scheme.

Control Scheme

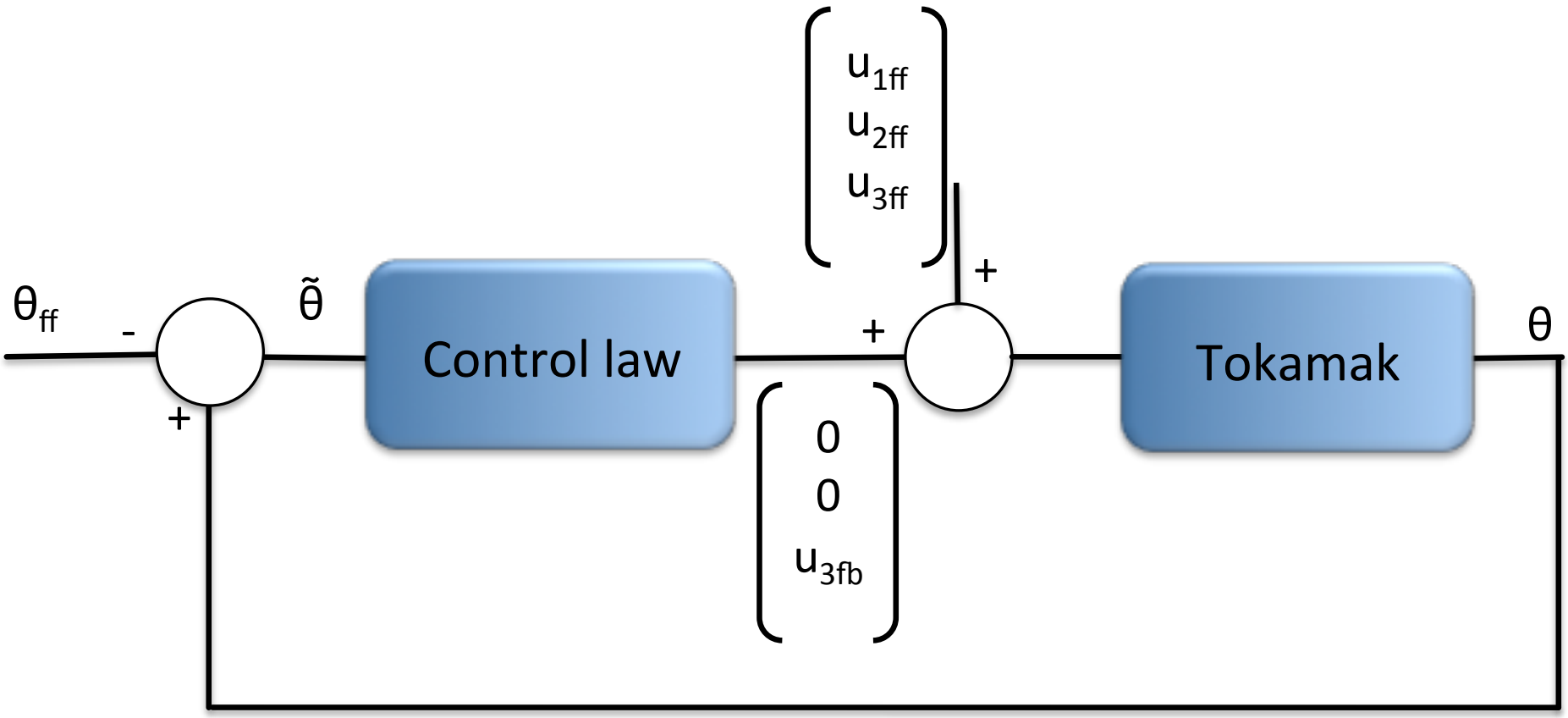

Figure: Feedback control scheme.

- A backstepping technique is used to obtain a control law for u_{3fb}.
- The feedback term compliments the feedforward inputs to ensure that θ profile tracks the nominal profile θ_{ff}.

Backstepping Controller Design

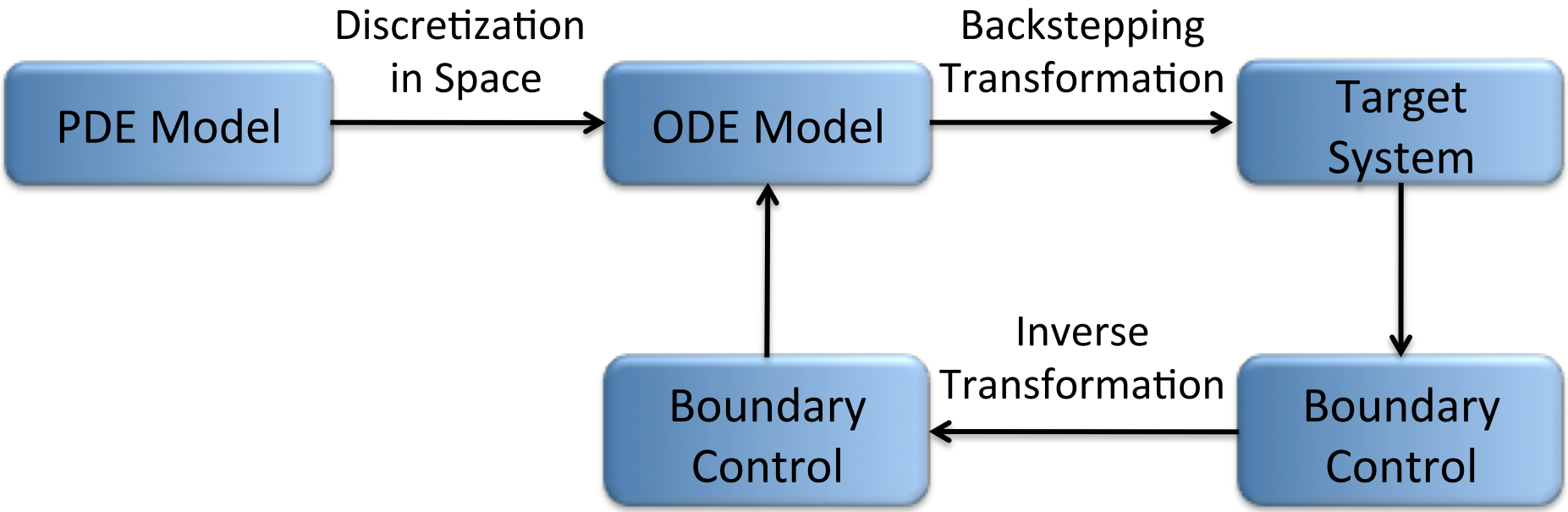

Figure: Schematic of backstepping technique.

- The backstepping technique provides a recursive method for finding a boundary condition control law that transforms the original system into a chosen target system.
- The stability and performance of the closed loop system can be altered through the choice of the target system.

Backstepping Transformation

ODE Model $\rightarrow$ Target System

$$\dot{\tilde{\theta}}^i = h_0^i u_{1\,ff} \frac{\tilde{\theta}^{i+1} - 2\tilde{\theta}^i + \tilde{\theta}^{i-1}}{h^2} + h_1^i u_{1\,ff} \frac{\tilde{\theta}^{i+1} - \tilde{\theta}^{i-1}}{2h} + h_2^i u_{1\,ff} \tilde{\theta}^i \quad (9)$$

$$\tilde{\theta}^N = -k_3 u_{3\,fb} \quad (10)$$

$$\dot{\tilde{w}}^i = h_0^i u_{1\,ff} \frac{\tilde{w}^{i+1} - 2\tilde{w}^i + \tilde{w}^{i-1}}{h^2} + h_1^i u_{1\,ff} \frac{\tilde{w}^{i+1} - \tilde{w}^{i-1}}{2h} + h_2^i u_{1\,ff} \tilde{w}^i - C_w^i u_{1\,ff} \tilde{w}^i \quad (11)$$

$$\tilde{w}^N = 0 \quad (12)$$

- We find a transformation of the form

$$\tilde{w}^i = \tilde{\theta}^i - \alpha^{i-1}(\tilde{\theta}^0, \ldots, \tilde{\theta}^i - 1)$$

by subtracting (11) from (9) and solving for α^i.

Backstepping Transformation

- We obtain the formula

$$\alpha^i = -\left[\frac{1}{\frac{h_0^i}{h^2} + \frac{h_1^i}{2h}}\right]\left[\left(\frac{-2h_0^i}{h^2} + h_2^i - C_w^i\right)\alpha^{i-1} + \left(\frac{h_0^i}{h^2} - \frac{h_1^i}{2h}\right)\alpha^{i-2} - \frac{1}{u_{1_{ff}}}\dot{\alpha}^{i-1} + C_w^i\tilde{\theta}^i\right] \tag{13}$$

  where $\dot{\alpha}^{i-1}$ is calculated as

$$\dot{\alpha}^{i-1} = \sum_{k=1}^{i-1}\frac{\partial\alpha^{i-1}}{\partial\tilde{\theta}^k}\dot{\tilde{\theta}}^k \tag{14}$$

- Expression (13) can be recursively evaluated at each node of the discretization scheme, starting with $\alpha^0 = 0$.

Boundary Condition Control Law

- The boundary condition control law is found by subtracting (12) from (10) and solving the resulting expression for $u_{3\,fb}$:

$$u_{3_{fb}} = -\frac{1}{k_3}\alpha^{N-1} \tag{15}$$

- The expression α^{N-1} is a linear function of the measurements of $\tilde{\theta}$ at each of the interior nodes that can be evaluated offline to obtain a static state feedback control law.

$$u_{3\,fb} = -K\Theta \tag{16}$$

where K is a row of controller gain values and Θ is a vector of error measurements.

Nonlinear Transformation of Inputs

- After adding the feedback term to the feedforward input ($u_3 = u_{3\,ff} + u_{3\,fb}$), the I_p, P_{tot}, and n requests, which are sent to existing dedicated controllers, are determined by the nonlinear transformations

$$I_p = u_3 \tag{17}$$

$$P_{tot} = u_3^2 u_{2_{ff}}^2 \tag{18}$$

$$\bar{n} = u_{1_{ff}}^{2/3} u_3^2 u_{2_{ff}} \tag{19}$$

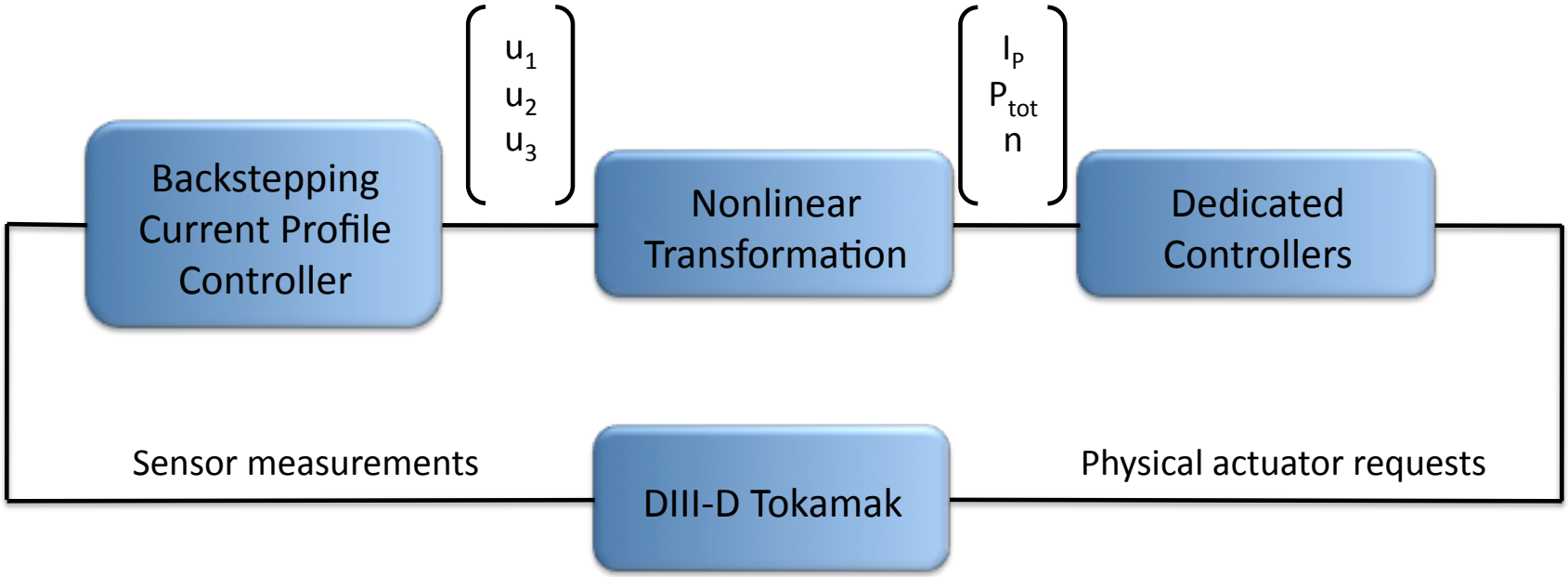

Stability of the Target System

- The discretized target system is a linear time-varying system and can be written in matrix form as

$$\dot{\beta}(t) = (M - \mathbf{C_w})\,\beta(t) u_{1_{ff}}(t) \tag{20}$$

- β is a vector of the target system states, $\mathbf{C_w}$ is a square matrix with the design parameters C_w^i along its diagonal, and the system matrix M depends on the model parameters.
- Since $u_{1\,ff}(t) > 0$, stability of the system is achieved as long as $(M - \mathbf{C_w})$ is negative definite.
- For the model parameters used in this work, M is negative definite, so, the design parameters C_w^i are chosen to improve the speed of response of the system and add robustness to disturbances.

Controller Test Shots

- In one shot, a particular set of feedforward inputs was used to to generate a target θ evolution
- In a second shot, an input bias was added to the feedforward inputs to artificially create profile perturbations and disturbances
- As part of testing, the controller and disturbances were turned on and off according to the timeline below

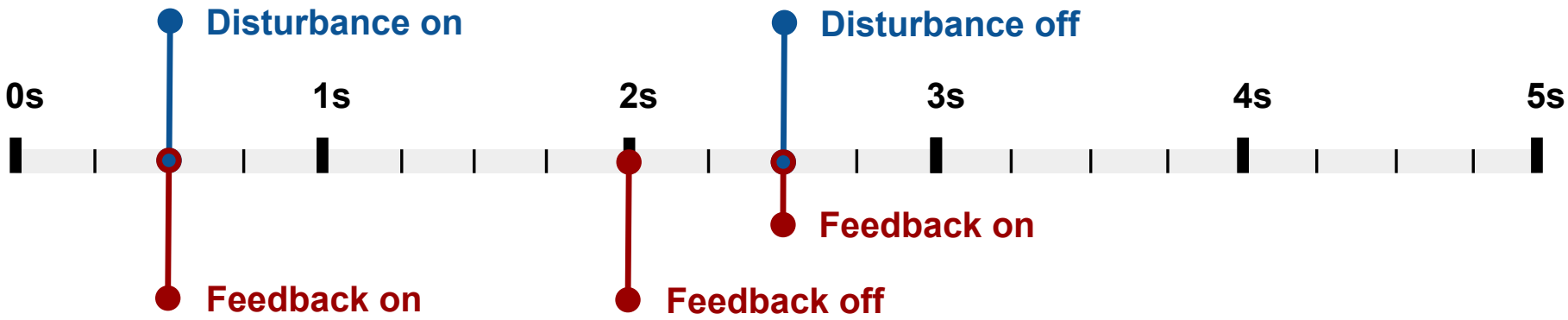

Figure: Timeline of controller test shot.

Simserver Simulation

- Prior to experimental testing, a simserver simulation study was done
- The simserver architecture allows the PCS to receive simulated data and provide control commands to a simulation model
- This enabled us to tune the controller design and debug the implementation of the algorithm

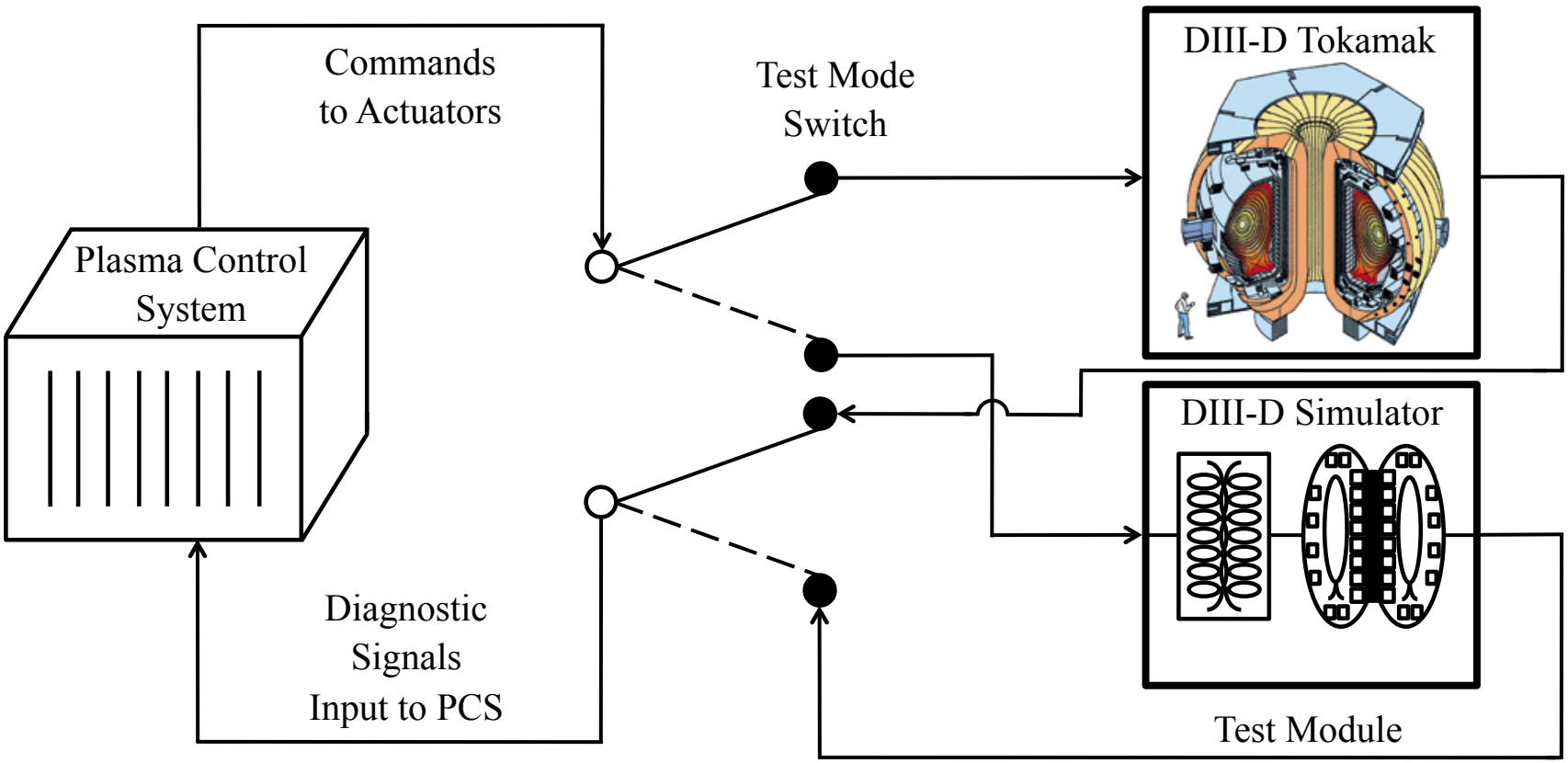

Simulation Results - Time Traces

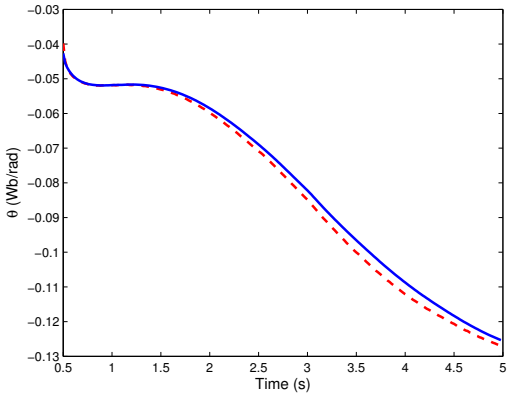

(a) $\hat{\rho} = 0.1$

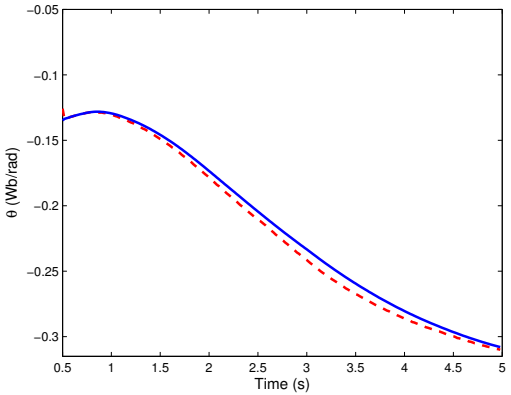

(b) $\hat{\rho} = 0.25$

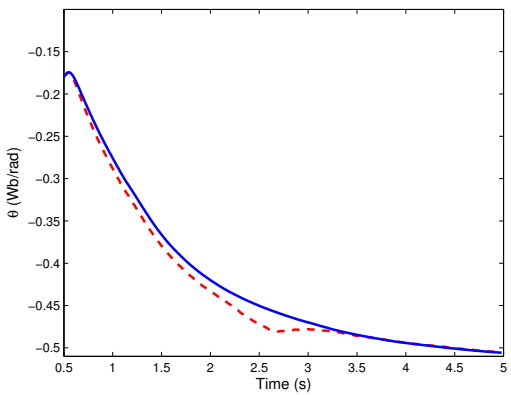

(c) $\hat{\rho} = 0.5$

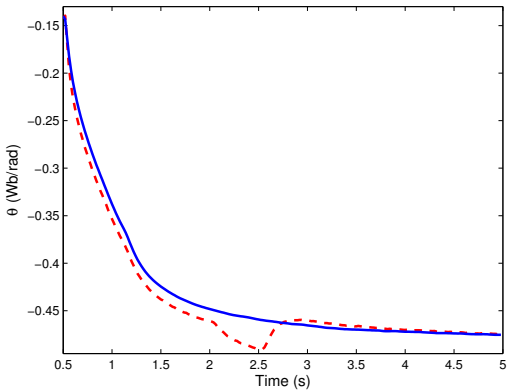

(d) $\hat{\rho} = 0.65$

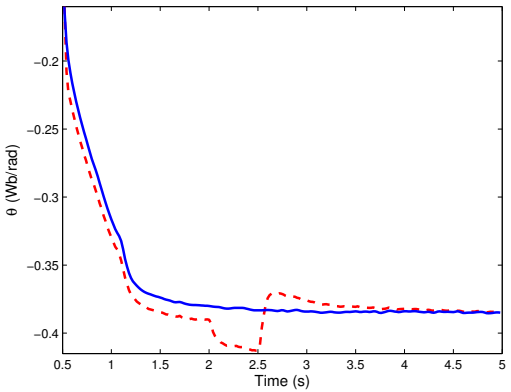

(e) $\hat{\rho} = 0.8$

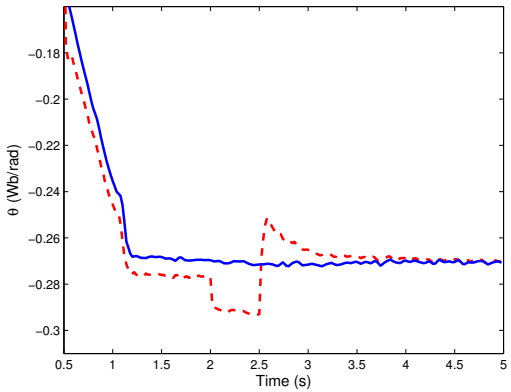

(f) $\hat{\rho} = 0.95$

Figure: Time trace of θ at various points comparing the target (blue-solid) and the closed loop, disturbed simulation (red-dashed).

Simulation Results - Profiles

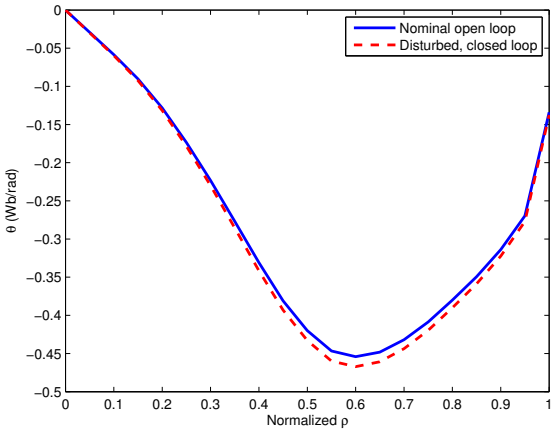

(a) $t = 2.00$s **(control on)**

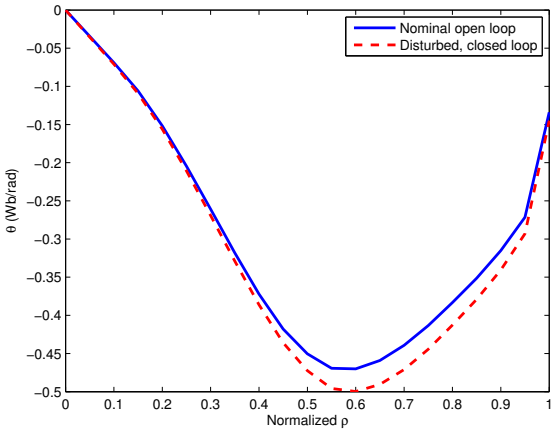

(b) $t = 2.5$s **(control off)**

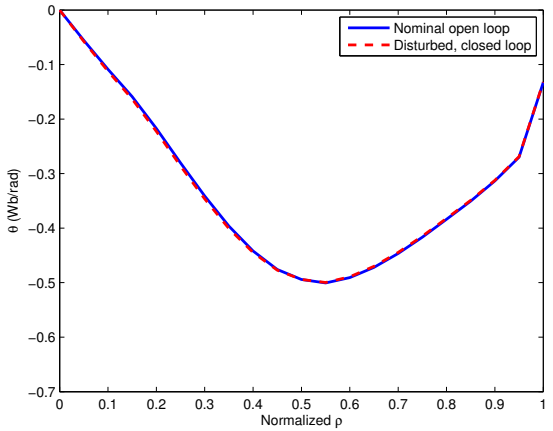

(c) $t = 4.00$s **(control on)**

Figure: Comparison of θ profiles at various times for the target (blue-solid) and the closed loop, disturbed case (red-dashed). Partial disturbance rejection is seen in (a), the effect of the uncontrolled disturbance can be noted in (b), and the recovery of the target profile after the disturbance is removed and the controller is turned back on can be observed in (c).

Simulation Results - Actuators

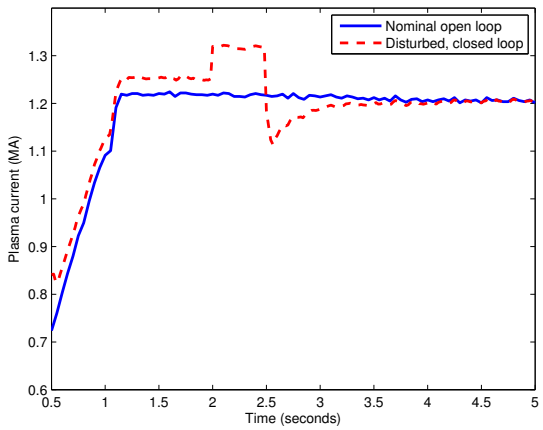

(a) Plasma current I_p

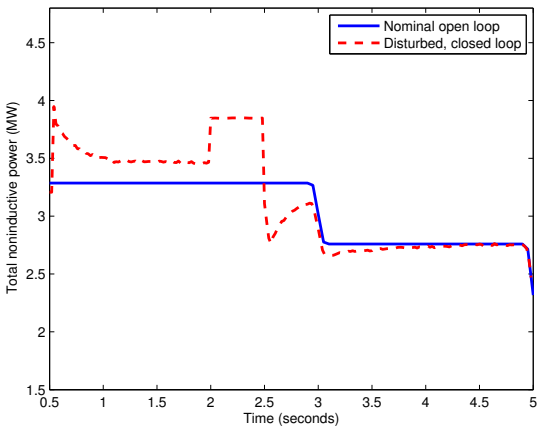

(b) Non-inductive power P_{tot}

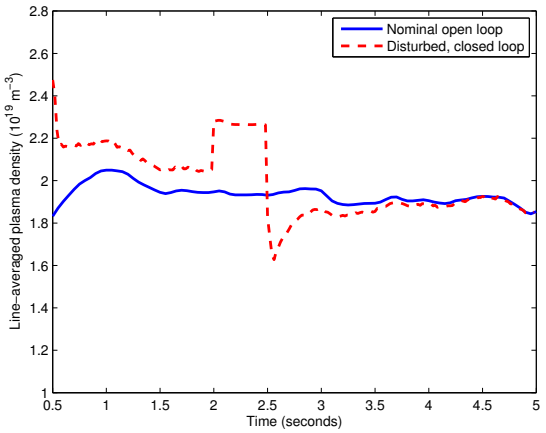

(c) Line averaged density $\bar{n}$

Figure: Comparison of actuators during the nominal simulation and the closed loop, disturbed simulation.

Experimental Results - Time Traces

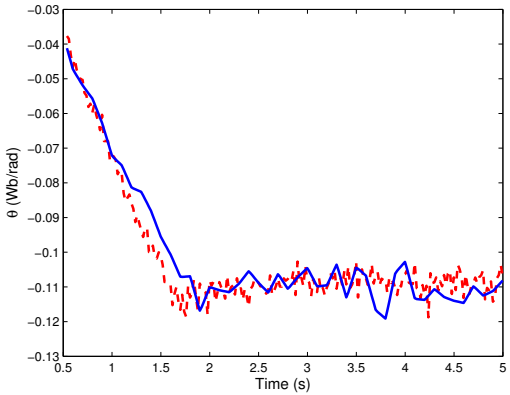

(a) $\hat{\rho} = 0.1$

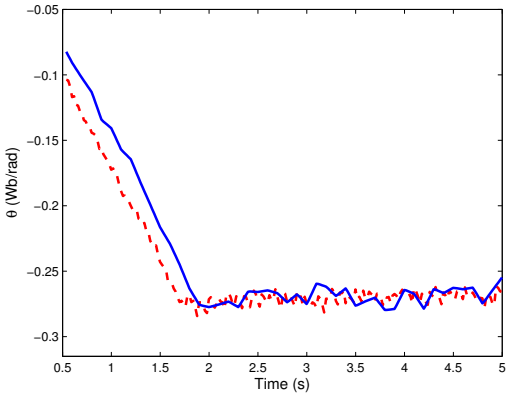

(b) $\hat{\rho} = 0.25$

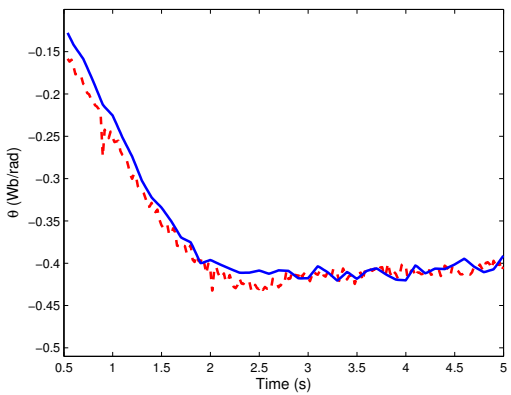

(c) $\hat{\rho} = 0.5$

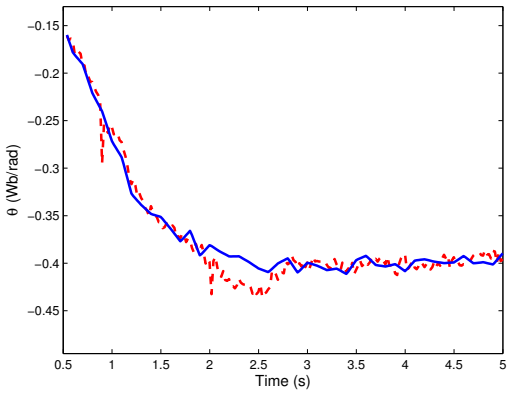

(d) $\hat{\rho} = 0.65$

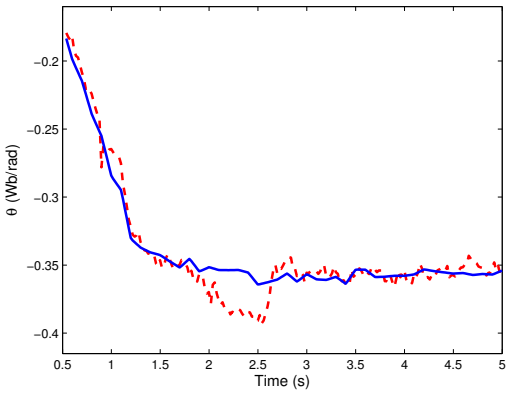

(e) $\hat{\rho} = 0.8$

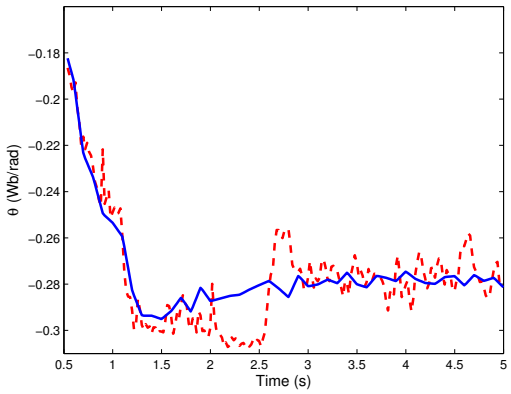

(f) $\hat{\rho} = 0.95$

Figure: Time trace of θ at various points comparing the reference shot 145477 (blue-solid) and the closed loop, disturbed shot 146454 (red-dashed).

Experimental Results - Profiles

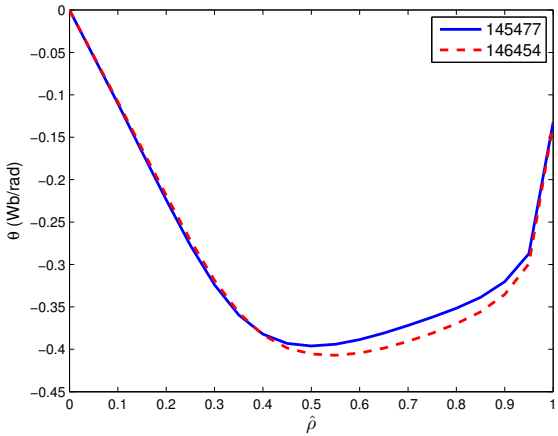

(a) $t = 2.00$s **(control on)**

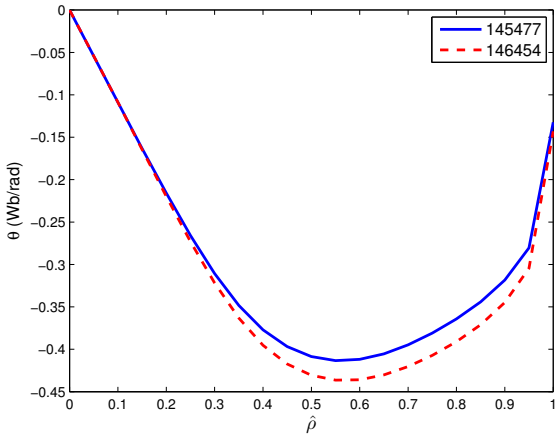

(b) $t = 2.50$s **(control off)**

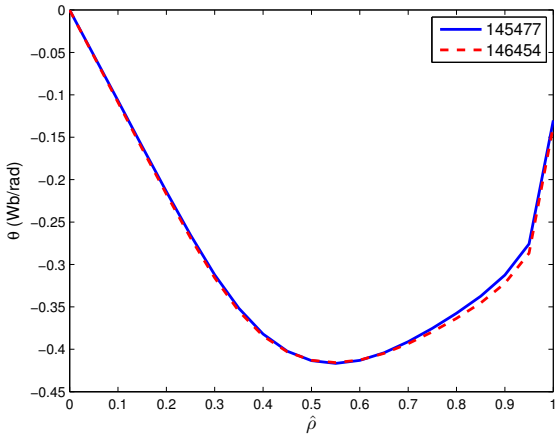

(c) $t = 4.00$s **(control on)**

Figure: Comparison of θ profiles at various times for reference shot 145477 (blue-solid) and the closed loop, disturbed shot 146454 (red-dashed). Partial disturbance rejection is seen in (a), the effect of the uncontrolled disturbance can be noted in (b), and the recovery of the target profile after the disturbance is removed and the controller is turned back on can be observed in (c).

Experimental Results - Actuators

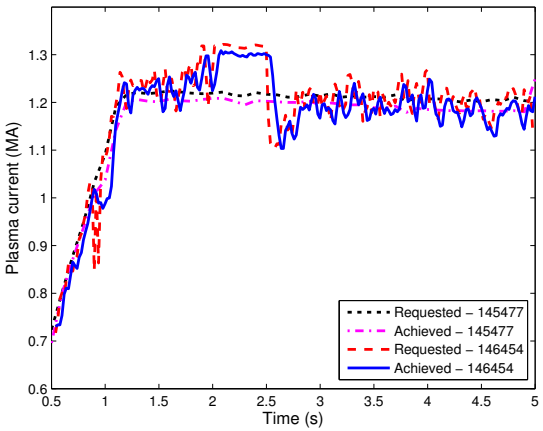

(a) Plasma current I_p

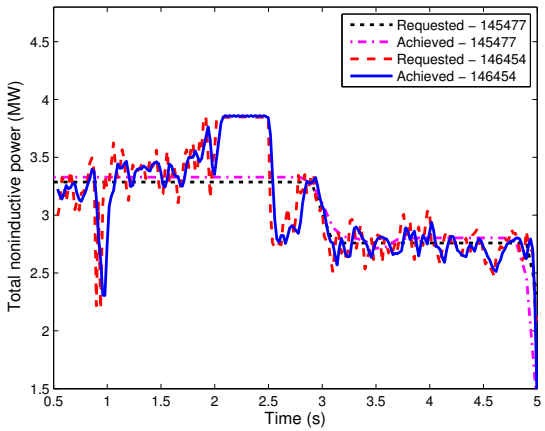

(b) Non-inductive power P_{tot}

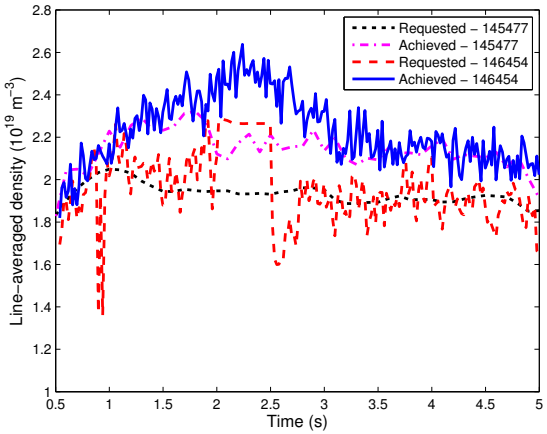

(c) Line averaged density $\bar{n}$

Figure: Comparison of requested and achieved actuator values during the reference shot 145477 and the closed loop, disturbed shot 146454.

Discussion and Future Work

Discussion

- With the controller turned on, the effect of the input disturbance is reduced as compared to when it is turned off
- A certain amount of steady state error can be seen when the disturbance is present, which is not unexpected since the controller is static
- When the disturbance is turned off, the controller quickly returns the profile to the target

Future work

- We plan to add **more feedback terms** ($u_{1\,fb}$, $u_{2\,fb}$) for further performance improvement
- **Integral action** will be added to improve disturbance rejection
- The technique will eventually be applied to an **H-mode discharge**